J. Phytol. Res. **38**(2): 149-164, 2025 **ISSN 0970-576**

EXPLORING THE ADSORPTIVE INTERACTION BETWEEN *BAUHINIA TOMENTOSA* LEAVES POWDER AND METHYL RED DYE: AN ISOTHERMAL KINETIC STUDY AND GREEN SYNTHESIS OF SILVER NANOPARTICLES FROM ITS LEAVES EXTRACT

CASANDRA GAONA[1], SAPNA SHARMA[2], RICHA THAWANI[2] and EKTA MENGHANI[3*]

[1] Autonomous University of the State of Hidalgo, Mexico.
[2] Department of Chemistry, JECRC University, Jaipur, Rajasthan, India.
[3]Department of Biotechnology, JECRC University, Jaipur, Rajasthan, India
*** Corresponding Author's Email:** ekta.menghani@jecrcu.edu.in

In this work, *Bauhinia tomentosa* leaves were used as a biosorbent that can remove methyl red dye from aqueous solutions. Pseudo-first-order and pseudo-second-order models were used to assess adsorption kinetics, and Langmuir and Freundlich isotherms were used to analyze equilibrium data. The results indicate that the adsorption process follows the Langmuir isotherm. The system fitting the Langmuir isotherm model indicates that adsorption occurs on a uniform surface with a finite number of identical sites. Besides, the Langmuir constant R_L value is ranged between 0 and 1, confirming favorable adsorption the maximum adsorption capacity found to be 9.699 mg/g for *Bauhinia tomentosa* leaves powder. The best fit was given by the pseudo-second-order kinetic model and displayed higher correlation coefficients. Additionally, silver nanoparticles were synthesized using the extract of the *Bauhinia tomentosa* leaves, exhibiting a significantly higher removal efficiency of methyl red compared to the plant-based biosorbent. These results highlight *Bauhinia tomentosa's* leaves extract shows potential as an environmentally friendly method of producing nanoparticles for wastewater treatment applications, as well as a sustainable biosorbent.

Keywords: Adsorption, *Bauhinia tomentosa*, Isothermal studies, Methyl Red Dye, Kinetic studies, and Silver Nanoparticles.

Introduction

Over time, contamination from dyes has been increasing. This causes great effects on both the environment and human health. Among these dyes, Methyl Red (MR), a widely used azo dye in the textile and pharmaceutical industries, is a toxic, mutagenic, or carcinogenic water pollutant when discharged without treatment[1]. Traditional processes have many limitations, such as low efficiency, high cost, and by-products[2]. In recent years, the utilization of biosorbents derived from plant materials has emerged as a promising, eco-friendly,

Received: 15 July,2025 *Revised: 26 October,2025* *Accepted: 31 December,2025*

and cost-effective alternative for dye removal. Adsorption, as one of the most effective methods for wastewater treatment, has been successfully applied to reduce hazardous inorganic/organic pollutants present in the effluents[3]. Among various plant species, *Bauhinia tomentosa* L (belonging to the family Fabaceae) commonly known as the There could be an addition like te family of the plant Yellow Orchid Tree, possess tremendous antimicrobial property and widely available in Asian countries like India and Sri Lanka, Zimbabwe and Mozambique[4].

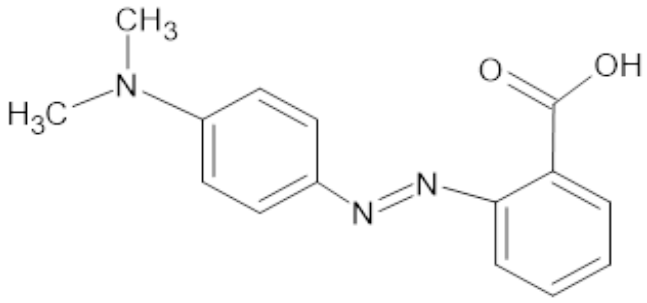

Figure 1. Chemical structure of Methyl Red Dye.

The investigation of *Bauhinia tomentosa* leaves powder as an adsorbent enhances the expanding research on natural plant-based materials for environmental remediation. In addition, another approach was used, which is using *Bauhinia tomentosa* leaves extracts for silver nanoparticles synthesis that enables an eco-friendly, economical, and straightforward process, avoiding the use of toxic chemical agents.

The present study focuses on evaluating the efficacy of *Bauhinia tomentosa* leaf powder as a biosorbent for the removal of Methyl Red dye from aqueous solutions, as well as the synthesis of silver nanoparticles.

Material and Methods

Various instruments employed in this work were Touchscreen Analytical Balance (WENSAR), Digital pH meter (Electronics India Alpha 01), UV-Visible Spectrophotometer (Analytical Double Beam UV 3200 Spectrophotometer, Labindia), Mini Rotary Shaker (Remi RS 12R), Laboratory water bath, and Magnetic stirrer with heating plate.

Preparation of Adsorbate (Methyl Red Dye solution)

A stock solution of 100 ppm was prepared by mixing 0.1 g of methyl red dye (MR) (analytical grade) and distilled water in a volumetric flask of 1 L, taking care to shake the flask very well so that the MR dissolves. Subsequently, 100 ml dilutions were prepared with concentrations of 10, 20, 30, 40 and 50 ppm from the stock solution. The physical characteristics of MR dye (Figure 1) are given in Table 1.

Table 1: Physical characteristics of Methyl Red dye.

Property	Value
Name	Methyl Red / 2-(N,N-dimethyl-4-aminophenyl)azobenzenecarboxylic acid
Molecular Formula	$C_{15}H_{15}N_3O_2$
Molecular Weight / g mol^{-1}	269.30
State	Crystalline Solid
Melting Point / °C	179 – 182

Preparation of Adsorbent (Bauhinia tomentosa leaves powder)

1. The *Bauhinia tomentosa* leaves were collected from campus area of JECRC University (Jaipur Engineering College and Research Center University located in Jaipur, Rajasthan) in month of June 2025 (10 June 2025) during summer season in afternoon time (10 am).
2. Mixed leaves were collected manually and then washed two times with tap water followed by washing two times with distilled water to remove impurities.
3. These leaves (5 g) then shade dried at room temperature for 3 days (approximately 30 °C)
4. Once the leaves were completely dried, they were ground to fine consistency using mortar and pestle, without employing any solvent during the process.
5. The powder obtained was named as *Bauhinia tomentosa* leaves Powder (BTLP) and stored in an air tight bottle until required for adsorption experiments. Till then no other physical and chemical treatments were done.

Adsorption studies

100 ml Erlenmeyer flask was utilized to carry out batch sorption experiments in which 0.20 g of the biosorbent, *Bauhinia tomentosa* leaves Powder (BTLP) and 50 ml of MR dye solution (10 – 50 ppm) at a pH of 4.1 were added at 30°C.

The Erlenmeyer flasks were agitated in a shaker at 180 rpm for 3 hours to achieve equilibrium. UV-Visible spectrophotometer for MR dye is used to determine concentrations of dye in the solution after equilibrium adsorption at 426 nm.

The equilibrium adsorption capacity, denoted as q_e (mg/g), was determined using eq. 1:

$$q_e = \frac{(C_o - C_e) * V}{W} \quad \ldots\ldots\ldots\ldots\ldots\ldots\ldots (1)$$

In this expression, C_o and C_e represent the initial and equilibrium concentrations of the dye in the solution (mg/L), V is the total volume of the dye solution in liters (L), and W corresponds to the weight of the adsorbent applied (g).

To evaluate the adsorption process over time, kinetic experiments were performed at different concentrations of methyl red (MR). The adsorption capacity at a specific time t, q_t (mg/g), was calculated based on eq. 2:

$$q_t = \frac{(C_o - C_e) * V}{W} \quad \ldots\ldots\ldots\ldots\ldots\ldots (2)$$

The percentage of dye removed from the solution was calculated using eq. 3:

$$\%\, removal = \frac{(C_o - C_e)}{C_o * 100} \quad \ldots\ldots\ldots\ldots\ldots\ldots (3)$$

To analyze the adsorption behavior, both Langmuir[16] and Freundlich[17] isotherm models were applied. Additionally, the kinetics of the process were examined through pseudo-first-order and pseudo-second-order models.

Synthesis of silver nanoparticles based on Bauhinia tomentosa leaves extract

Desired amount of silver nitrate (analytical grade) were weighed and mixed it with distilled water in a 500 ml volumetric flask to prepare 1mM silver nitrate ($AgNO_3$) , making sure to reach the fill line. Then it was wrapped in aluminum foil to avoid direct sunlight.

Leaves from the *Bauhinia tomentosa* plant were collected, washed with distilled water, and cut into smaller pieces. These were placed in Erlenmeyer flasks with 250 ml of distilled water. One flask was placed in a hot bath at a temperature between 50 and 60°C, while the other flask was placed on a hot plate at a temperature range between 70 and 80°C. All flasks were heated for 30 min.

After this time, the flasks were allowed to cool for a first filtration with filter paper followed by another with Whatman filter paper.

Table 2: Composition of Silver Nitrate solution and plant extract.

1:1	10 ml $AgNO_3$ + 10 ml plant extract
1:2	10 ml $AgNO_3$ + 20 ml plant extract
2:1	20 ml $AgNO_3$ + 10 ml plant extract

The extracted obtained was put in contact with the silver nitrate solution using the following ratios as given in Table 2.

The addition of the silver nitrate solution should be slow. Therefore, in conical flasks the plant extract was taken and while the addition of silver nitrate was done through burette (drop by drop). During this process, the flask was heated at 70-80°C in constant agitation.

Results and Discussion

Determination of λ_{max}

λ_{max} for MR dye was obtained by the Analytical Double Beam UV 3200 Spectrophotometer. A graph was plotted of absorbance versus wavelength and the dye exhibited maximum absorption at 426 nm and shown in Figure 2.

Calibration curve

Absorbance readings were taken for each of the 10, 20, 30, 40 and 50 ppm solutions at λ_{max} in order to construct a calibration curve of Absorbance vs Concentration (Figure 3). The resulting calibration curve is used to determine MR concentration samples by measuring their absorbance and locating the corresponding concentration on the curve.

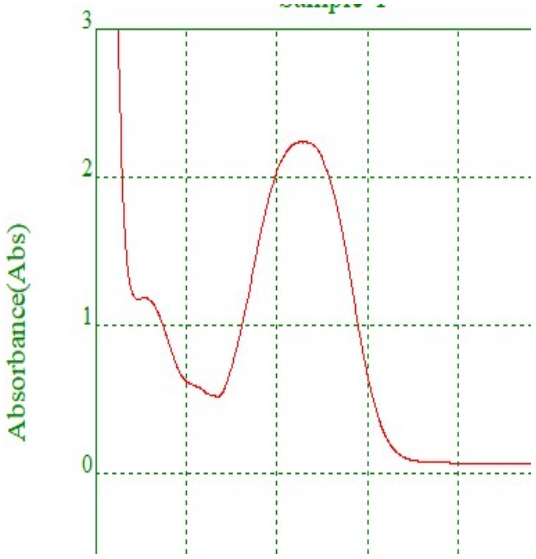

Figure 2. Absorbance and wavelength

Effect of initial dye concentration

The effect of initial MR concentration (10 – 50 ppm) on the intake rate of MR by BTLP with an adsorbent dosage of 0.20 g and mixing speed of 180 rpm was studied and shown as in Figure 4 by plotting a graph between concentrations of adsorbate vs time. Absorbance readings were taken every 30 minutes during 3 hours. The amount of MR dye absorbed at equilibrium (q_e) increased from 0.559 to 2.391 mg/g as the concentration of dye was increased from 10 to 50 ppm. That is because as the initial concentration increases more dye molecules are available in the solution, and although a portion of them is adsorbed onto the surface, not all of them can be captured due to the saturation of active sites. As a result, the amount of unabsorbed dye left in solution at equilibrium (C_e) increases[5,6].

Table 3: Langmuir and Freundlich model constants and correlation coefficients for biosorption of MR by BTLP.

Isotherm	Parameters
Langmuir isotherm	
Q_o (mg/g)	9.699321
b (L/mg)	0.007818
R^2	0.993
R_L	0.720236
Freundlich isotherm	
K_F	0.097471
n	1.154068
R^2	0.9995

Table 4: Percentage removal of MR dye with/without AgNPs.

Agitation time (h)	% Removal (with AgNPs)	% Removal (without AgNPs)
0.5	8.528965	8.461409
1.0	27.00557	11.16365
1.5	35.17987	15.38591
2.0	50.75156	18.59483
2.5	57.67607	20.45263

The MR removal decreased from 22.22% to 19.25% as concentration was increased from 10 to 50ppm. Equilibrium concentrations were

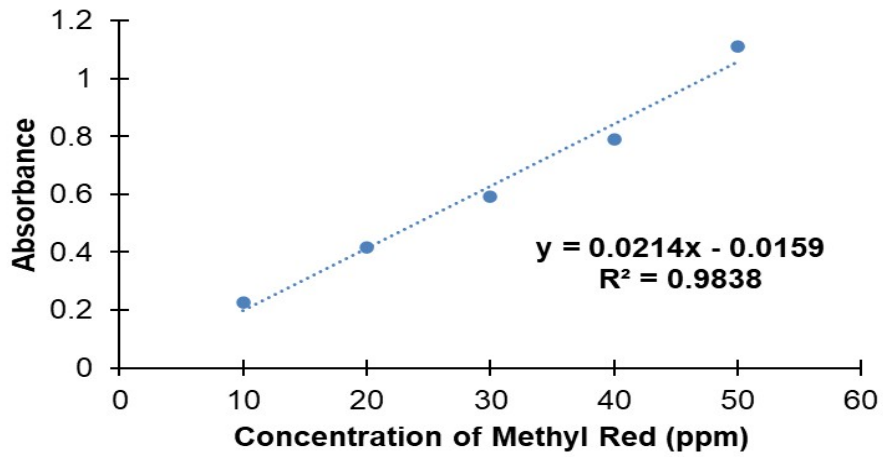

Figure 3. Calibration curve between concentrations of MR dye and absorbance (showing verification of Lambert Beers Law)

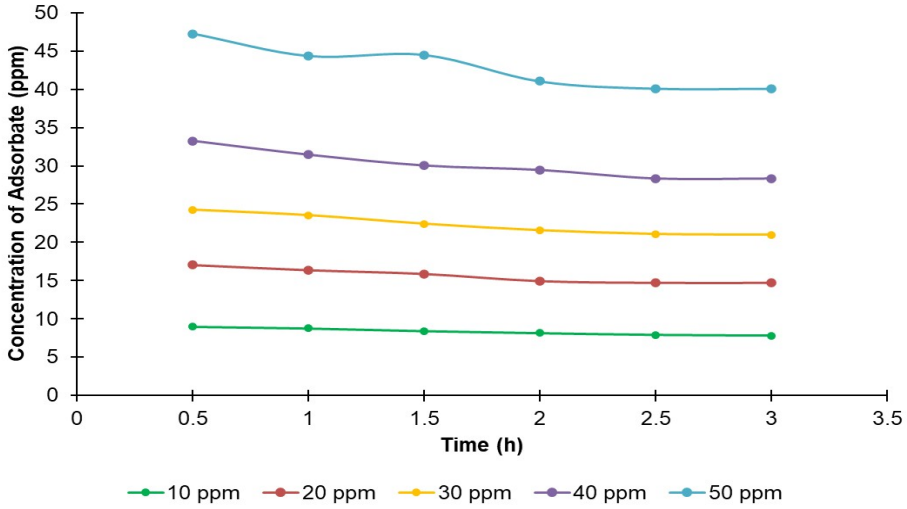

Figure 4. Graph between concentrations of adsorbate with time interval to show effect of initial dye concentration on removal of MR by BTLP

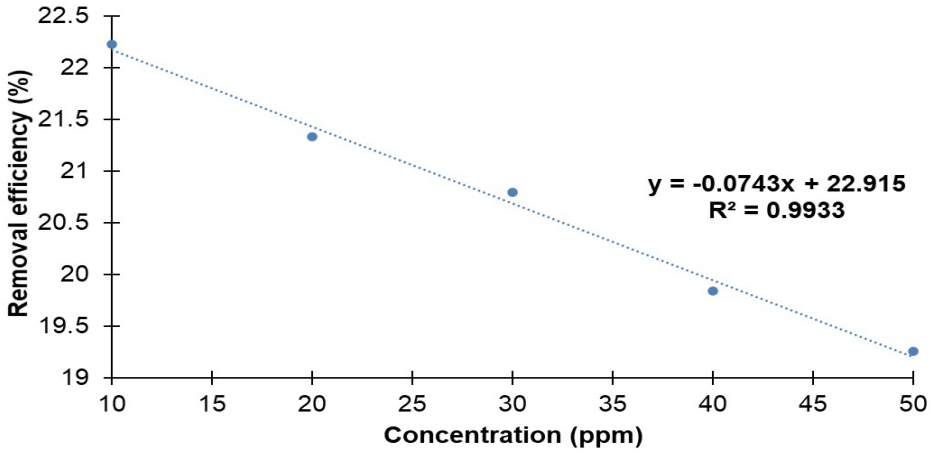

Figure 5. Graph between removal efficiency and concentration of dye to show percentage removal of MR by BTLP

reached within 3 hours. Figure 5 shows the plot between initial dye concentration and the percentage of dye removed. At higher concentrations, the adsorbent becomes saturated with adsorbate molecules, so percentage removal decreases[7].

Effect of biosorbent dose

The adsorbent dose factor is important for determining the capacity of a biosorbent because it directly influences the amount of contaminant that can be removed from a solution. The experiments were conducted with constant dye concentration (40 ppm) and samples of biosorbent dosages ranging from 0.2 to 0.8 g under a constant temperature of 30°C and at a pH of 4.1 for 3 h.

It was observed that the percentage of dye adsorption increased with adsorbent dose. Specifically, from 19.83% to 29.57% when the biosorbent dose was increased from 0.2 to 0.8 g (Figure 6). This is because a higher biosorbent dose provides a larger surface area and increases the availability of binding sites, which can improve removal efficiency[8,9].

The plot shows that as the mass of *Bauhinia tomentosa* leaves powder increases, its ability to purify the aqueous solution of methyl red dye also increases. This result indicates that the biosorbent has a direct relationship between its mass and adsorption capacity. Similar trends have been observed in studies using other biosorbents, such as *Rumex abyssinicus*[10], *Ceiba pentandra* L.[11], *Ulva lactuca*, *Corallina officinalis*[12], and banana peel[13].

Effect of agitation time

Equilibrium studies were carried out by adding a fixed amount of biosorbent (0.2 g) to 40 ppm dye solution at pH of 4.1 at 30°C (Figure 7). The flasks were agitated in a shaker at 180 rpm for 3 hours. Aliquots were taken at different times (0.5, 1.0, 1.5, 2.0, 2.5, 3.0 h) for the absorbance measurement. The plot shows that increasing the contact time, percentage removal of dye increases.

On increasing agitation time from 0.5 to 3.0 h, percentage removal of dye increased from 5.93% to 18.84% and correspondingly, equilibrium concentration C_e decreased from 33.27 ppm to 28.35 ppm. When contact time is longer, dye molecules have more opportunity to come into contact with the surface of the adsorbent, leading to a greater number of collisions between adsorbate and adsorbent[14,15].

Adsorption Isotherms

Adsorption isotherms establish a relationship between the concentration of adsorbate in the solution and the quantity adsorbed onto the surface. In this study, the experimental data were evaluated using the Langmuir and Freundlich isotherm models. The Langmuir adsorption model[16] assumes monolayer adsorption, where the surface of the adsorbent becomes fully covered by a single layer of solute molecules, without any interaction between them once adsorbed. This model is represented by eq. 4:

$$q_e = \frac{(Q_o b C_e)}{(1 + bCe)} \quad \ldots\ldots\ldots\ldots\ldots\ldots \quad (4)$$

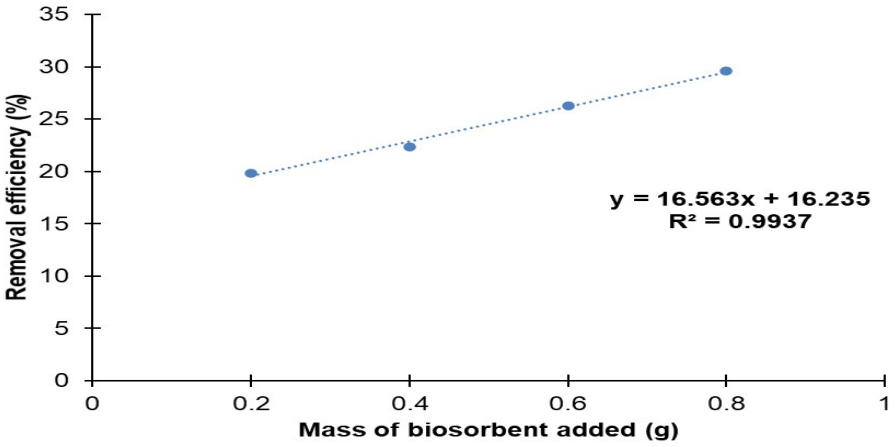

Figure 6. Graph between removal efficiency and mass of adsorbent added to show effect of Biosorbent Dosage (g) on percentage removal of MR by BTLP.

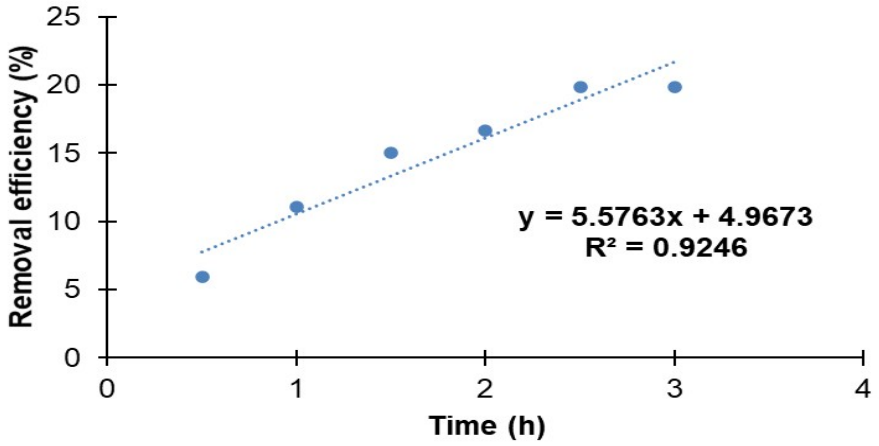

Figure 7. Graph between removal efficiency and time intervals to show effect of Agitation time on percentage removal of MR by BTLP.

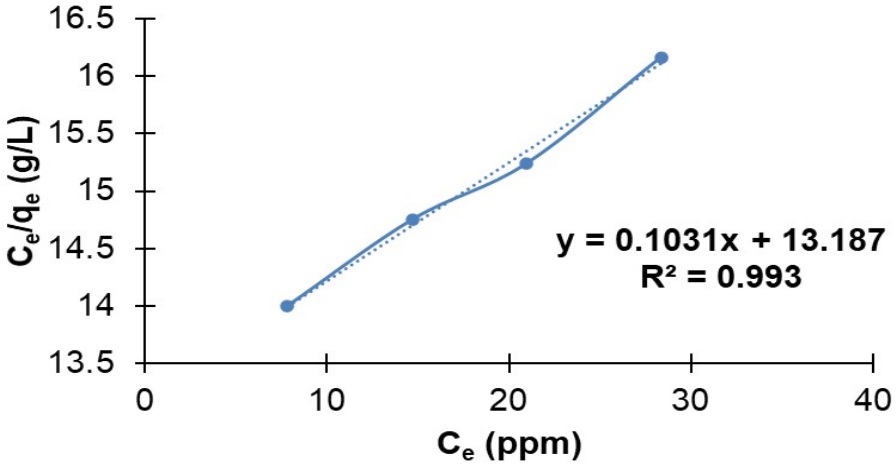

Figure 8. Langmuir isotherm for MR sorption onto BTLP at 30˚C.

In this equation, q_e (mg/g) denotes the amount of dye adsorbed per gram of adsorbent, while C_e (mg/L or ppm) is the dye concentration remaining in the solution at equilibrium. Q_0 corresponds to the maximum adsorption capacity forming a complete monolayer on the adsorbent surface at high C_e, and b (L/mg) is a constant reflecting the affinity between dye molecules and active binding sites. The Langmuir model can also be expressed in its linearized form.

$$\frac{C_e}{q_e} = \frac{1}{Q_0} + \frac{C_e}{Q_o} \quad \text{.....(5)}$$

A straight-line plot was obtained by graphing the equilibrium concentration (C_e) vs the ratio C_e/q_e (Figure 8), confirming the applicability of the Langmuir isotherm. From the slope and intercept of this linear relationship, the Langmuir constants Q_0 and b were calculated. The maximum adsorption capacity (Q_0) was determined to be 9.10 mg/g.

An important feature of the Langmuir isotherm is the dimensionless separation factor R_L which is defined by eq. 6:

$$R_L = \frac{1}{1 + bQ_0} \quad \text{.....(6)}$$

In this expression, C_0 represents the highest initial dye concentration (mg/L or ppm), and b is the Langmuir constant (L/mg). The R_L value helps classify the nature of the adsorption process as unfavorable ($R_L > 1$), linear ($R_L = 1$), favorable ($0 < R_L < 1$), or irreversible ($R_L = 0$).

The value of R_L was in the range of $0 < R_L < 1$, indicating favorable linear adsorption of MR onto BTLP. The value of correlation constant (R^2) according to the Langmuir isotherm comes out to be 0.993 and the maximum adsorption capacity found to be 9.699 mg/g for BTLP.

The Freundlich isotherm[17], describes a heterogeneous system by eq. 7. The Freundlich equation is expressed as:

$$q_e = K_F C_e^{1/n} \quad \text{..... (7)}$$

Where K_F and n are constants. K_F (mg/g $(L/mg)^{1/n}$) is the adsorption capacity of the sorbent and n gives an indication of the favorability of the adsorption process. Values of $n > 1$ represent favorable adsorption conditions[18]. To determine the constants K_F and n, the linear form of the equation was used to produce a graph of ln (q_e) against ln (C_e) as in Figure 9. Values of K_F and n are calculated from the intercept and slope of the plot given by eq. 8:

$$ln\, q_e = ln\, K_F + \left(\frac{1}{n}\right) \ln C_e \quad \text{.....(8)}$$

The value of R^2 according to the Freundlich isotherm comes out to be 0.9995. According to the results, both models fit the system. Although the Langmuir model has a relatively lower R^2 value than the Freundlich model, the R_L value demonstrate favorable adsorption. Therefore, the Langmuir isotherm show representative model for the system.

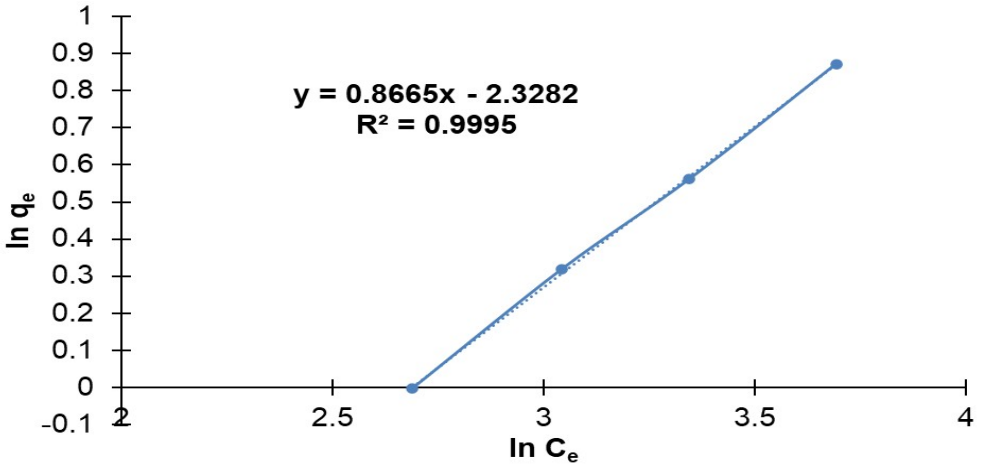

Figure 9. Freundlich isotherm for MR sorption onto BTLP at 30˚C.

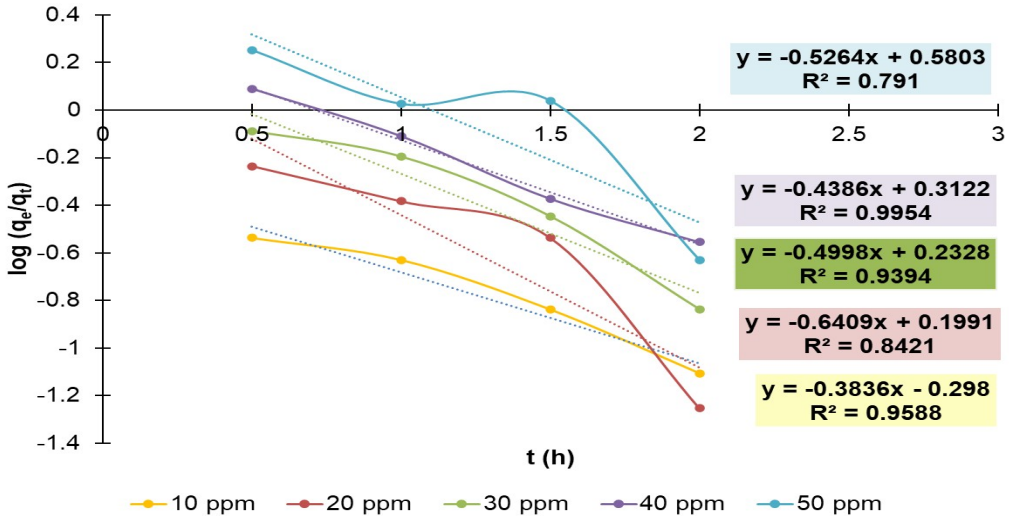

Figure 10. Pseudo first order sorption kinetics of MR onto BTLP.

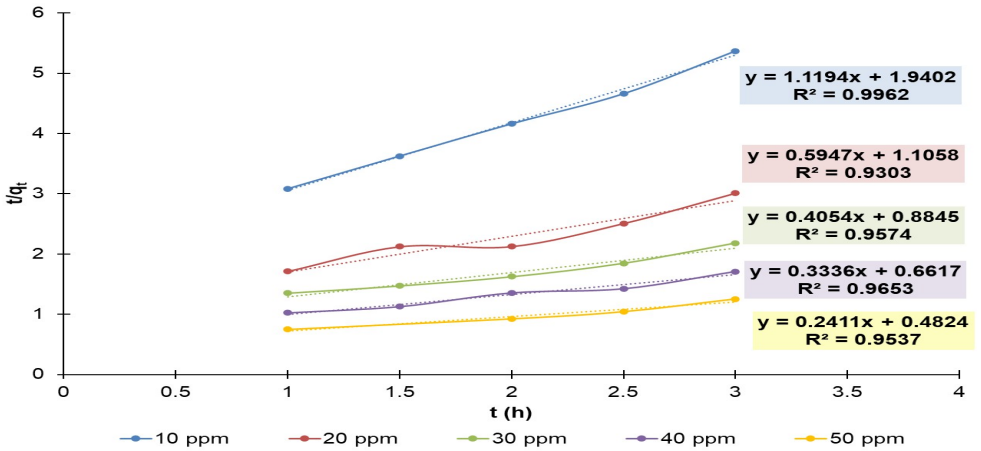

Figure 11. Pseudo second order sorption kinetics of MR onto BTLP.

The values of all constants are given in Table 3.

Adsorption Kinetics

A linear form of pseudo-first-order kinetics[19] is given by Lagergren:

$$log\ (q_e - q_t) = log\ q_e - \left(\frac{k_1}{2.303}\right)t$$

……..(9)

By plotting log ($q_e - q_t$) versus time, a straight line can be obtained, from which the rate constant was derived (Figure 10). A strong linear fit with a high correlation coefficient suggest that the process follows Lagergren's pseudo-first-order kinetic model. Consequently, this would imply that the adsorption mechanism corresponds to first-order kinetics[19]. The values of the rate constant k_1 and the equilibrium adsorption capacity q_e, as calculated from the model, are shown in Table 3 along with their respective correlation coefficients.

However, a noticeable discrepancy was observed between the experimental q_e values and those predicted by the model, indicating that the adsorption of methyl red (MR) does not conform to a pseudo-first-order kinetic behavior.

Alternatively, the pseudo-second-order model[20] is represented in its linear form by eq. 10:

$$\frac{t}{q_t} = \frac{1}{k_2 q_e^2} + \frac{1}{q_e}.t$$

……(10)

In this case, the slope and intercept of the plot of t/q_t vs t (Figure 11) were used to determine the equilibrium adsorption capacity q_e and the rate constant k_2 (g/mg·h).

The values of k_2 and q_e determined from the model with their corresponding correlation coefficients. There is better agreement in terms of correlation coefficient values (R^2) for the pseudo second order model (R^2=0.9605) tan for the pseudo first order model (R^2=0.9053). Hence, the pseudo second order model better represents the adsorption kinetics.

Color change during synthesis of silver nanoparticles

The formation of silver nanoparticles (AgNPs) from *Bauhinia tomentosa* leaves extract was indicated by the color shift from yellow/orange to brown that was seen during the synthesis process [21,22]. It can be observed that the solution shows an absorption peak around ~410 nm, which was attributed to the presence of silver nanoparticles. In Figure 12, a noticeable color change was observed between the original plant extract solution (a) and the liquid phase silver nanoparticles (AgNPs) synthesized from the extract (b) as shown in Figure 13.

The bioactive components of the *Bauhinia tomentosa* extract, including flavonoids, phenolic acids, and tannins, function as natural reducing agents when silver nitrate ($AgNO_3$) is added.

Silver nanoparticles are created and grow as a result of these phytochemicals reduction of silver ions (Ag^+) from silver nitrate into metallic silver (Ag^0).

$$AgNO_3 \xrightarrow{plant\ extract} AgNPs + Oxidized\ phytochemicals$$

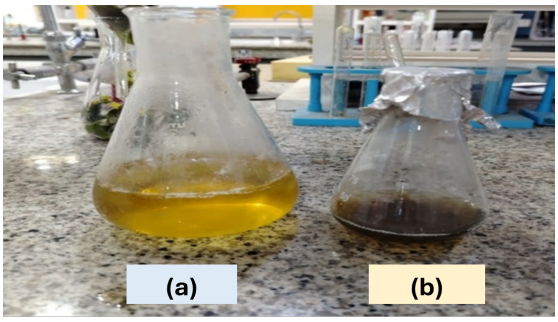

Figure 12. Plant extract: (a) without AgNPs and (b) with AgNPs.

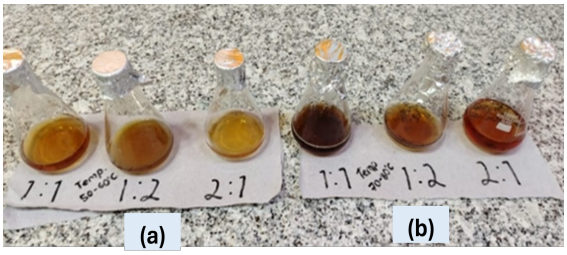

Figure 13. Liquid phase AgNPs derived from *Bauhinia tomentosa* leaves extract: (a) 50-60^{0}C and (b) 70-80^{0}C. *(color change in different composition of silver nitrate and plant extract solution at two different temperatures)*

The phenomenon known as surface plasmon resonance (SPR), which happens when conduction electrons on the surface of silver nanoparticles resonate with incident light, is responsible for the brown appearance[23].

This visual alteration is a first indication that the nanoparticles have formed successfully.

Evaluation of MR adsorption with AgNPs and BTLP

To make a comparison of MR dye adsorption between the biosorbent BTLP and the silver nanoparticles, 5 ml of the 2:1 solution that was heated in the range of 70-80°C was taken, along with 50 ml of the 30 ppm MR solution. Then, absorbance values were measured every ~30 min, obtaining the following results for percentage removal of MR dye (Table 4).

A linear plot (Figure 14) allows to compare the removal efficiency of both materials through time. It can be observed that the silver nanoparticles show higher dye removal efficiency, with a maximum absorption of 57.67%, while the BTLP biosorbent exhibits lower efficiency, with a value of 20.79% for 30 ppm MR dye solution. Therefore, silver nanoparticles offer a greater advantage in selecting the best adsorbent for the removal treatment of methyl red (MR).

According to other studies, there was a significant difference in the percentage of removal achieved by silver nanoparticles compared to other types of biosorbents. A 2022 study synthesized a gum-katira–AgNP composite (6–20 nm particles) and tested it on methyl red dye showing 95.7% removal under optimized conditions[24]. In one of the another study[25], AgNPs were created within a chitosan/PVA matrix where they achieved 85% removal of methyl red dye and 77% for methylene blue. Suyambumani et al.[26] perform phytochemical analysis of *Bauhinia tomentosa* leaves extract and show the presence of flavonoids, alkaloids, phenols, saponins, terpenoids, tannins, starch, and steroids. The presence of various phytochemical constituents not only contributes to its bioactivity but also play a significant role in the adsorption process through interactions with target contaminants[27].

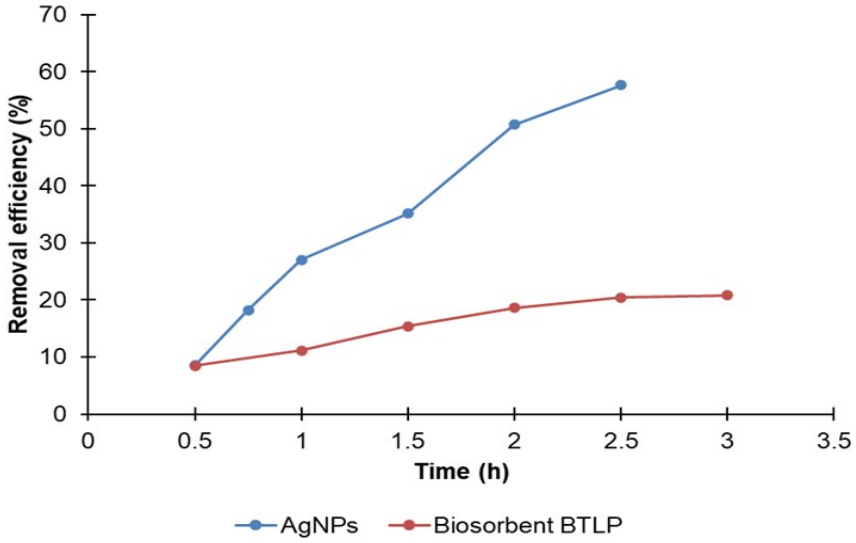

Figure 14. Percentage removal of MR by with and without AgNPs.

Conclusion

Kinetic and isotherm studies were conducted to evaluate the adsorption behavior of a biosorbent derived from *Bauhinia tomentosa* leaves powder for the removal of methyl red dye. Based on the data analysis, the adsorption process was found to conform more closely to the Langmuir isotherm model (R^2=0.993), despite the fact that the Freundlich model exhibited a slightly higher R^2 value (0.9995). The applicability of the Langmuir model is supported by the calculated R_L value (0.720237), which ranged between 0 and 1, indicating favorable adsorption.

Furthermore, kinetic modeling revealed that the pseudo-second-order model provided a better fit for the experimental data (Mean R^2=0.9605), as evidenced by higher correlation coefficients compared to the pseudo-first-order model (Mean R^2=0.9050).

This means the process is specific, uniform, chemically driven, and limited to a single layer of adsorption ideal characteristics for effective and reliable wastewater treatment.

In addition to the biosorbent study, silver nanoparticles (AgNPs) were successfully synthesized using the extract of *Bauhinia tomentosa* leaves extract. These AgNPs demonstrated significantly higher dye removal efficiency (57.67%) compared to the leaves powder biosorbent (20.45%) for 30 ppm dye solution, suggesting that the nanomaterial offers enhanced potential for application in dye-contaminated wastewater treatment.

Overall, this research underscores the dual potential of *Bauhinia tomentosa* both as a sustainable biosorbent and as a natural precursor of green source for nanoparticle synthesis. The findings provide strong basis for advancing cost-effective, eco-friendly materials for the treatment of dye-laden and industrial effluents .materials for the treatment of dye-laden and industrial

effluents. Future investigations on scale-up, reusability, and performance with real wastewater are essential to transform these encouraging laboratory findings into viable environmental remediation strategies.

References

1. Alharbi AA, Aldaghri O, El-Badry BA, Ibnaouf K, Alfadhl F, Albadri A, Ahmed AH, and Modwi A 2024, Degradation of Methyl Red (MR) dye via fabricated Y_2O_3–MgO/g-C_3N_4 nanostructures: Modification of band gap and photocatalysis under visible light. *Optical Materials* **152** 115443.
2. Periyasamy AP 2024, Recent Advances in the Remediation of Textile-Dye-Containing Wastewater: Prioritizing Human Health and Sustainable Wastewater Treatment. *Sustainability* **16**(2) 495
3. Ruan W, Hu J, Qi J, Hou Y, Zhou C, and Wei X 2019, Removal of dyes from wastewater by nanomaterials: A review. *Advanced Materials Letters* **10**(1) 9-20.
4. Sharmila G, Pradeep RS, Sandiya K, Santhiya S, Muthukumaran C, Jeyanthi J, Kumar NM and Thirumarimurugan M 2018, Biogenic synthesis of CuO nanoparticles using *Bauhinia tomentosa* leaves extract: Characterization and its antibacterial application. *Journal of Molecular Structure* 1165 288-292.
5. Ding Y, Liu Y, Liu S, Li Z, Tan X, Huang X, Zeng G, Zhou ,Y Zheng B and Cai X 2016, Competitive removal of Cd (II) and Pb (II) by biochars produced from water hyacinths, performance and mechanism. *RSC Advances* **6** 5223–5232.
6. Santhi T, Manonmani S and Smitha T 2010, Removal of methyl red from aqueous solution by activated carbon prepared from the *Annona squmosa* seed by adsorption. *Chemical Engineering Research Bulletin*, **14**(1) 11-18.
7. Asadullah M, Ain Q and Ahmad F 2022, Investigation of a Low Cost, Stable and Efficient Adsorbent for the Fast Uptake of Cd (II) from Aqueous Media. *Advanced Journal of Chemistry* **5**(4) 345-356.
8. Rudi N N, Muhamad M S, Chuan L T, Alipal J, Omar S, Hamidon N, Hamid N H A, Sunar N M, Ali R and Harun H 2020, Evolution of adsorption process for manganese removal in water via agricultural waste adsorbents. *Heliyon* **6**(9) e05049.
9. Amorim D, Costa B and Martinez D 2023, Biosorption of Pd (II) from Aqueous Solution using Leaves of *Moringa oleifera* as a Low-cost Biosorbent. *Bioactivities* **1**(1) 9-17.
10. Abewaa M, Adino E and Mengistu A 2023, Preparation of *Rumex abyssinicus* based biosorbent for the removal of methyl orange from aqueous solution. *Heliyon*, **9**(12) e22447.
11. Zein R, Fathony H, Ramadhani P and Deswati D 2023, Facile chemically activation process of kapok husk as a low-cost biosorbent for removal methylene blue dye in aqueous solution. *Journal of the Serbian Chemical Society* **89**(1) 123-140.
12. Ameen MM, Moustafa AA, Mofeed J, Hasnaoui M, Olanrewaju OS, Lazzaro U and Guerriero G 2021, Factors Affecting Efficiency of

Biosorption of Fe (III) and Zn (II) by Ulva lactuca and Corallina officinalis and Their Activated Carbons. *Water* **13**(23) 3421.
13. Farias K C S, Guimarães R C A, Oliveira K R W, Nazário C E D, Ferencz J A P and Wender H 2023, Banana Peel Powder Biosorbent for Removal of Hazardous Organic Pollutants from Wastewater. *Toxics* **11** 664.
14. Sharma P, and Kaur H 2011, Sugarcane bagasse for the removal of erythrosin B and methylene blue from aqueous waste. *Applied Water Science* **1**(3-4) 135-145.
15. Fito J, Abewaa M, Mengistu A, Angassa K, Ambaye A D, Moyo W, and Nkambule T 2023, Adsorption of methylene blue from textile industrial wastewater using activated carbon developed from Rumex abyssinicus plant. *Scientific Reports* **13**(1).
16. Eastoe J and Dalton J 2000, Dynamic surface tension and adsorption mechanisms of surfactants at the air–water interface. *Advances in Colloid and Interface Science*, **85**(2-3) 103-144.
17. Freundlich H M1906, Over the Adsorption in Solution. *Journal of Physical Chemistry A* **57** 385-470.
18. Poots V J P, Mckay G and Healy J J 1978, Removal of basic dye from effluent using wood as an adsorbent. *J. Water Pollut. Control Fed*. **50** 926–935.
19. Lagergren S 1898, About the Theory of So-Called Adsorption of Soluble Substances. Kungliga Svenska Vetenskapsakademiens *Handlingar* **24** 1-39.
20. Ho Y S and McKay G 1998, Sorption of Dye from Aqueous Solution by Peat. *Chemical Engineering Journal* **70** 115-124.
21. Shahzadi S, Fatima, S, Ain Q U, Shafiq Z and Janjua M R S A 2025, A review on green synthesis of silver nanoparticles (SNPs) using plant extracts: a multifaceted approach in photocatalysis, environmental remediation, and biomedicine. *RSC Advances* **15**(5) 3858-3903.
22. Fahim M, Shahzaib A, Nishat N, Jahan A, Bhat T A and Inam A 2024, Green Synthesis of Silver Nanoparticles: A Comprehensive Review of Methods, Influencing Factors, and Applications. *JCIS Open* **16** 100125.
23. Jayanti P D, Zurnansyah N, Kusumah H P, Mahardhika L J, Riswan M, Wahyuni S, Adrianto N, Cuana R, Istiqomah N I, Ali H, Ali D, Chotimah N and Suharyadi E 2024, Localized Surface Plasmon Resonance Properties of Green Synthesized Ag/rGO Composite Nanoparticles Utilizing Amaranthus Viridis Extract for Biosensor Applications. *Journal Of Science Advanced Materials and Devices* **9**(3) 100747.
24. Asmare Z G, Aragaw B A, Atlabachew M and Wubieneh T A 2022, Kaolin-Supported Silver Nanoparticles as an Effective Catalyst for the Removal of Methylene Blue Dye from Aqueous Solutions. *ACS Omega* **8**(1) 480-491.
25. Meydan I, Aygun A, Tiri R N E, Gur T, Kocak, Y, Seckin H and Sen F 2023, Chitosan/PVA-supported silver nanoparticles for azo dyes removal: fabrication, characterization, and assessment of

antioxidant activity. *Environmental Science Advance* **3**(1) 28-35.

26. Suyambumani S, Pandiyan J, Wong L S, Djearamane S, Mathanmohun M and Sagadevan S 2024, Phytochemical analysis and antimicrobial potential of *Bauhinia tomentosa* leaf extracts. *Journal of Phytology* **16** 41-48
27. Balaji M, Senthilkumar P, Ravikumar L and Balakumaran M 2018**,** Green synthesis of silver nanoparticles (AgNPs) using *Bauhinia tomentosa* leaf extract and their photocatalytic activity. *Journal of Materials Science: Materials in Electronics* **29** 11509–11520.